Granular Matter (2016) 18:18
DOI 10.1007/s10035-016-0625-1

ORIGINAL PAPER

On the contact force distributions of granular mixtures under 1D-compression

N. H. Minh[1,2] · **Y. P. Cheng**[2]

Received: 4 July 2015 / Published online: 18 March 2016

Abstract We investigate the distribution of the inter-particle contact forces inside granular mixtures of a sand-particle-size material and of a finer-particle-size material using the Discrete Element Method for frictional spherical grains. The numerical granular samples were compressed vertically with no lateral expansion following a common stress path in soil mechanics; the material states varied from jammed states towards highly jammed states with increasing solid fraction. The inter-particle contacts were categorized depending on the particle sizes of the two contacting entities. The force distributions of the contact networks were calculated depending on the contact types. It was found that different contact networks possess a similar shape of the probability distribution function of the contact forces when the populations of the respective particle sizes are involved in the percolation of the strong forces in the systems. For systems of a small percentage of the fine particles, the fine particles do not actively participate in the strong force transmission and the related contact force distributions reflect the characteristic of an unjammed state for the subsystem consisted of these particles.

Keywords Granular mixtures · Discrete element · Strong force transmission · Contact force distribution · One dimensional compression

✉ N. H. Minh
minh.nguyen@nu.edu.kz

[1] School of Engineering, Nazarbayev University, Astana 010000, Republic of Kazakhstan

[2] Department of Civil, Environmental and Geomatic Engineering, University College London, Gower Street, London WC1E 6BT, UK

1 Introduction

The behaviour of granular materials is a common research topic in many areas of engineering and material sciences. In civil engineering, the granular behaviour of sandy soils is studied in which the investigations often consider the shear failure behaviour that occurs at large displacements, the compression of sands under an applied vertical (static) load and zero lateral expansion, and the liquefaction behaviour of the materials under a vibration (dynamic) condition during an earthquake. Under a constrained boundary condition, a granular sample can behave like a solid; the friction at inter-particle contacts can be utilized to provide an internal shear resistance to the forces and deformation applied from the boundaries. When shear stress exceeds the maximum internal shear resistance of granular soils, large shear displacements can take place and this can be amplified in an unconstrained condition where the materials can flow like a liquid as in an avalanche.

Similar to civil engineers, physicists [1–4] have studied the jamming transition of disordered materials where a jammed system can resist shear stresses and an unjammed system flows under any applied shear stresses. For athermal systems, a jammed state can be reached by increasing the system's density above a certain critical density value following an isotropic compression loading path, whereas unjamming of a lightly jammed system can be triggered by increasing the shear stresses applied on the system above the yield stress value at the current density. A shear-jamming phase diagram for athermal systems of frictional disks was proposed by Bi et al. [1], which was developed based on the original framework proposed earlier by Liu and Nagel [2], for systems jammed at densities less than the critical value. Materials below the critical density when subjected to pure shear strains from an isotropic stress state may undergo the jamming transition,

and this depends on the possibility of creating an anisotropic contact network. In shear-jammed states, forces applied at the boundaries of a system are transmitted across a granular material through a highly heterogeneous contact network consisting of two groups of strong and weak contacts that are classified based on the magnitude of the contact forces that they carry [1,5,6]. The strong contacts carry contact forces larger than the mean contact force value in a granular system and a shear-jammed state of a system of frictional grains would occur when the strong force network percolates in all directions [1]. Change in the probability distribution function (*pdf*) of contact forces from a monotonically decreasing distribution in a flowing regime (unjammed) to a distribution having a peak probability density near the mean contact force value was considered a structural signature of a jammed granular system [3].

Civil engineers often encounter many natural granular materials of a wide range of different particle size distributions (*psd*) and it has been shown that the *psd* is an important factor that controls both the macroscopic characteristics [7–10] and the microscopic characteristics [11–13] of a granular material. In this paper, we investigated the distributions of the inter-particle contact forces inside granular mixtures of a sand-particle-size material and of a finer-particle-size material (the maximum particle size ratio between the two materials was about 10) using the Discrete Element Method (DEM) for frictional spherical grains. The numerical granular samples were compressed vertically with no lateral expansion following a common one-dimensionally compression stress path in soil mechanics, in which shear stress increases proportionally with mean stress. The material states varied from jammed states towards highly jammed states with increasing solid fraction values. The inter-particle contacts were categorized depending on the particle sizes of the two contacting entities, and the force distributions of the contact networks of different contact types were calculated accordingly, following previous studies [12]. In this paper, we propose that different contact type networks possess a similar *pdf* shape when the populations of the respective particle subsystems actively participate in the percolation of the strong forces in the systems. For systems with a small percentage of the fine particles, the fine particles do not actively participate in the strong force transmission. The shape of the *pdf* curves of these small-small particles contacts, induced by the fine particles population, reflects the characteristic of an unjammed state for the subsystem consisted of these small-size fine particles.

2 Simulation procedures

The Itasca discrete element method (DEM) package [14], PFC3D, was used to simulate the one-dimensional compression behaviour of granular mixtures where numerical granular samples bounded by static rigid side walls were compressed in the vertical direction with no lateral expansion. The DEM granular mixture samples were created by mixing two component materials; one has the particle size distribution of a real sand ranging from $d_{min} = 0.4$ mm to $d_{max} = 1.2$ mm and the other material consisted of finer single-size-particles of $d_0 = 0.1$ mm diameter. The *psd*(s) of these two component materials (referred to as sand and fines) are shown in the inset of Fig. 1. The fines content (by mass) was varied in the range from 0, 10, 20 %, up to 100 %.

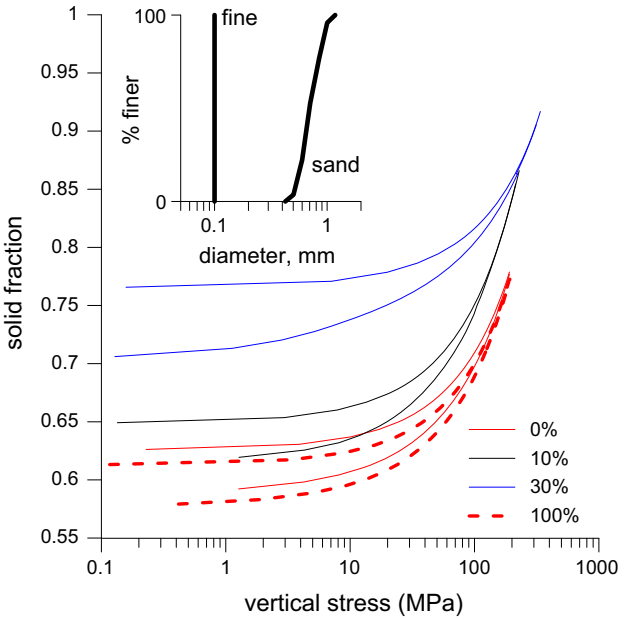

Fig. 1 One dimensional compression curves of different granular mixtures, the percentage values indicate the fines content; the *inset* shows the particle size distributions of the constituent materials in the mixtures

Spherical particles of different sizes were initially generated to form gas-like assemblies inside a cubical space bounded by frictionless walls. The initial particle systems were brought to a mean pressure of approximately 100 kPa with no gravity through an isotropic compression process. Dense samples and loose samples were created in this step using two inter-particle friction values of 0.0 and 0.5 respectively. Once the systems reached the specified mean stress, lateral walls were fixed in their current positions, the inter-particle friction was set to 0.5 and the samples were ready for one dimensional compression. Samples were compressed vertically using a constant-strain-rate of 10^{-6}/s such that the particles and the horizontal walls were moved toward the horizontal mid-plane in small loading increments with periodic relaxation. When each increment was completed the applied velocity was set to zero and the systems were cycled at constant volume until the unbalanced forces in the system became negligible (i.e. equilibrium). Intermediate saved

Table 1 Input parameters for 3D DEM simulations

Input parameters	Value
Particle density	2650 g/m^3
Particle friction, μ	0.5
Contact elastic modulus, E_c	1×10^9 N/m^2
Particle stiffness ratio, k_s/k_n	1.0
Wall friction, μ_{wall}	0.0
Wall stiffness, k_{wall}	100 × average particle stiffness

files were created at different stress and strain values and they were used to extract the contact force information for the analyses in this study.

The input parameters for the DEM simulations are listed in Table 1. The linear elastic contact model [14] with Coulomb friction was used for the inter-particle interactions. The contact particle stiffness was calculated based on a scaling relationship with the constant particle elastic modulus and the particle size.

A summary of the sample size and the number of particles is given in Table 2 for different fines content values; note that d $\geq d_{min} = 0.4$ mm are particles of the (big) sand material, whereas $d = d_0 = 0.1$ mm are particles of the fine material in the mixtures. Due to the very large numbers of particles in these samples, differential density scaling [14] was used to reduce the computational time. Further details of the DEM simulation procedures can be found in [12] and [14]. Figure 2 shows the mixture samples of 10 and 30 % under 5MPa vertical stress where the sand and the fine particles are shown in different colours and the difference of 20 % fines content provides the 30 % fines sample a much greater number of the fine particles that are able to fully fill the void spaces as different from the 10 % fines sample. The populations of the sand and the fine particles can be considered as two particle subsystems in a total granular mixture system. The macroscopic stress tensor of the mixture is dependent on the force transmissions between the particles from the same subsystem and across two subsystems as calculated in [12] as follows:

$$\sigma_{ij} = \sigma_{ij}^{b\_b} + \sigma_{ij}^{b\_s} + \sigma_{ij}^{s\_s} \quad (1)$$

where σ_{ij} is the overall stress tensor and $\sigma_{ij}^{b\_b}$, $\sigma_{ij}^{b\_s}$, $\sigma_{ij}^{s\_s}$ are the three component stress tensors calculated separately based on different contacts between big and big (sand) particles, big (sand) and small (fine) particles, and small and small particles, respectively.

3 Packing structures of granular mixtures

Figure 1 plots the compression curves of the solid fractions of granular mixtures against the applied vertical stresses following the common practice in soil mechanics. Both shear stress and solid fraction increased simultaneously under this typical loading condition. The compression curves of different fines contents in Fig. 1 follow a similar trend in that the curves of the loose and dense samples converge to a common potentially straight line in a semi-log plot at high stress values larger than 100 MPa. In soil mechanics (e.g. [8]) the slope of this line is called the compression index and it is used to calculate volume change of soil samples under compression.

As the one dimensional compression was started at a finite pressure value, the granular samples were initially in jammed states for both loose samples (having a lower initial solid fraction) and dense samples (having a higher initial solid fraction). The monodisperse granular samples of 100 % fines content started from the lowest initial solid fraction values of 0.58 (loose) and 0.61 (dense) compared to other mixtures (0, 10, and 30 % fines content). This compares very well to the results of the granular samples of frictional grains of the same 0.1 mm diameter at the jamming transition in [15]. The jamming transition of monodisperse frictionless spherical grains on the other hand occurs at a higher solid fraction value of approximately 0.64, which has been well reported in the literature (e.g., [15,16]). The initial solid fractions of the mixture samples, and even of the slightly polydisperse sand samples, are greater than the solid fraction of the 100 % fines content samples due to better packing efficiency. The fine particles inside the mixture samples can be located within the pores between the bigger sand particles and this improves packing efficiency. Figure 3 plots the initial solid fractions of dense samples in terms of the fines content values; the dense sample of 30 % fines content has the maximum packing efficiency in terms of the maximum initial solid fraction value. There are sufficient fine particles in this system to densely fill the pore spaces whereas the big particles are still located closely to each other; good packing efficiency was obtained for both populations of the fine particles and of the sand particles [10].

Chan and Ngan [17] studied experimentally the contact force distribution of deformable particles and suggested that the force distribution is strongly related to the packing structure but much less to the sphere sizes and the applied load. The correlation between the packing structure and the contact force distribution can also be revealed in the jamming transition of granular packing; as the granular behaviour transforms from a liquid-like behaviour to a solid-like behaviour, the contact force distribution changes from a monotonically decreasing distribution to a distribution having a peak probability density near the mean contact force value [3]. In this study, we found a correlation between the jamming of the fine particles subsystem and the force distributions of the contacts induced by these particles.

Table 2 Sample size and the number of particles for DEM mixtures

Fines content (0 %)	Initial sample size	d ≥ 0.4 (mm)	$d = 0.1$ (mm)	Total particles
0	20^3 (mm^3)	25318	0	25,318
10	7^3 (mm^3)	973	32754	33,727
20	7^3 (mm^3)	857	66294	67,151
30	7^3 (mm^3)	751	98950	99,701
40	7^3 (mm^3)	643	131605	132,248
50	7^3 (mm^3)	536	164261	164,797
70	7^3 (mm^3)	320	229573	229,893
80	7^3 (mm^3)	212	262229	262,441
90	7^3 (mm^3)	105	294885	294,990
100	3^3 (mm^3)	0	25783	25,783

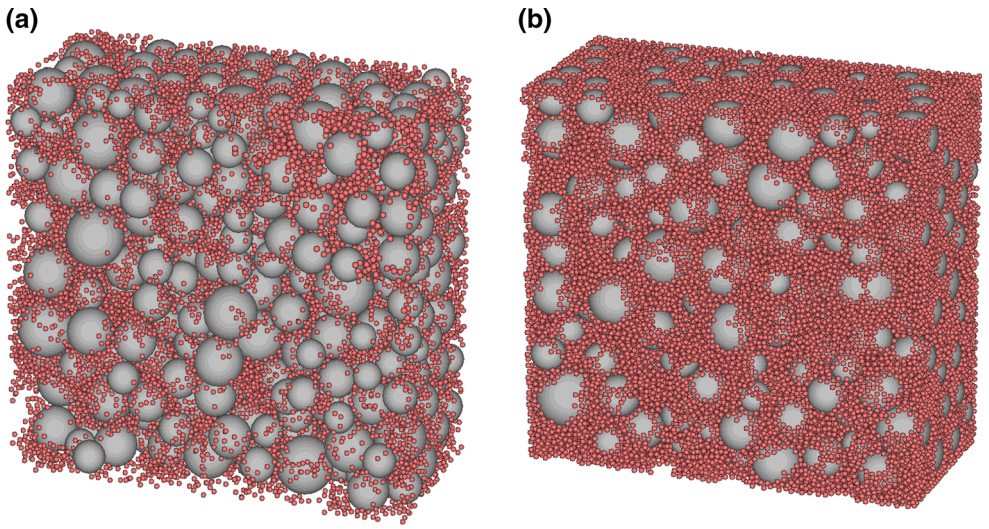

Fig. 2 Granular mixture samples of different fines contents at 5 MPa vertical stress; sand and fine particles are shown in different colours. **a** 10 % fines content, **b** 30 % fines content

3.1 Jamming of the fine particles subsystem and the non-rattler fraction

Bi et al. [1] studied the shear-jamming transition of frictional photoelastic disks and found that the transition was associated with the percolation of the strong force network. This depends on the fraction of the non-rattler particles in a granular system, where the non-rattler grains were defined as the ones carrying at least two force-bearing contacts [1]. A shear-jammed state was achieved when the strong force network percolated in all directions, attainable when the non-rattler fraction was equal or greater than 0.83. Study of systems of frictionless spherical particles [4] found a similar non-rattler fraction of 0.82 at the shear-jamming transition in three dimensional simulations. For the mixture systems of frictional spheres in this study, we propose an analogy between the percolation of the strong forces of the fine particles subsystem and the shear-jammed state of a full granular system.

To study the "jamming" of the fine particles fraction subsystem, we calculated the percentage of the fine particles as non-rattlers for 10, 30, and 100 % fines content samples where rattlers were particles having zero or one contact as these particles do not contribute to the stable state of stress [18]. In Fig. 4, the non-rattler percentages of both the dense and the loose samples of 100 % fines content are higher than the threshold value 83 %. For 30 % fines, the values are higher than 83 % when the vertical stresses are greater than 100 MPa. This is in the range where the compression curves converge in Fig. 1. For 10 % fines, the values are much lower than 83 % even at the end of the compression. Since the loading condition in this study is neither simple shear nor isotropic compression, and the fine particles only constitute a subsystem of the over mixtures the threshold value 83 % was only used here as a qualitative comparison. Nevertheless, the "jamming" of a granular (sub-)system can potentially be related to the non-rattler fraction. Further evidences are provided as follows.

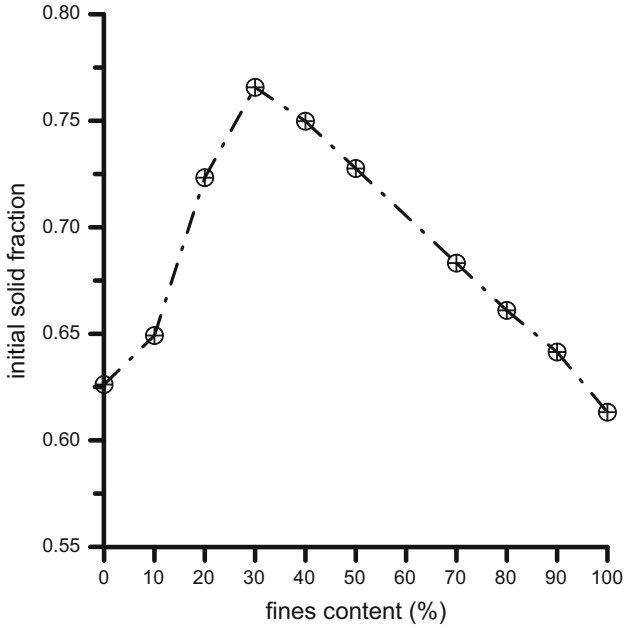

Fig. 3 Variation of the initial solid fraction depending on the fines content

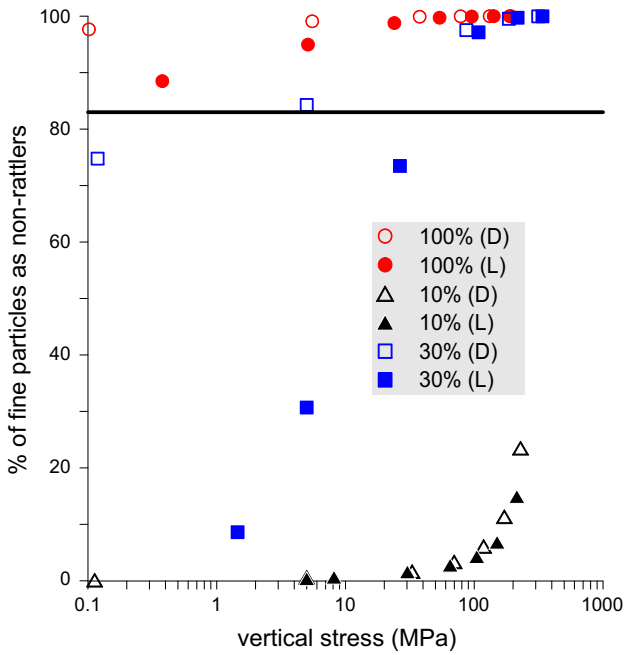

Fig. 4 Percentage of the fine particles that are non-rattlers in the systems where non-rattlers are defined as particles carrying at least two force-bearing contacts

The granular fine particles subsystems in the mixture samples are not in a jammed state if the fines content and the vertical stress/the solid fraction are low. This can be explained by revealing their package structures visually. Figures 5 and 6 show the locations of fine particles on a central vertical plane for the dense samples of 10 and 30 % fines contents respectively. The contact force transmitted through two contacting particles at the end of the one-dimensional compression, i.e. "high stress level" as shown in Fig. 1, is indicated as black lines connecting the centres of the two particles. Figure 5 shows that the black lines are scattered and unconnected; however, Fig. 6 shows that the black lines form percolated network with the sand particles. These figures confirm the observation in Fig. 4 where the fine particles in 10 % fines content sample are not jammed because they do not significantly transmit forces, whereas, for 30 % fines, they are jammed and hence transmit forces. The additional fine-fine particles contact forces in Fig. 6 actually contributes to the already percolated force network of the sand-sand particles contacts between the sample's boundaries (note, the sand par-

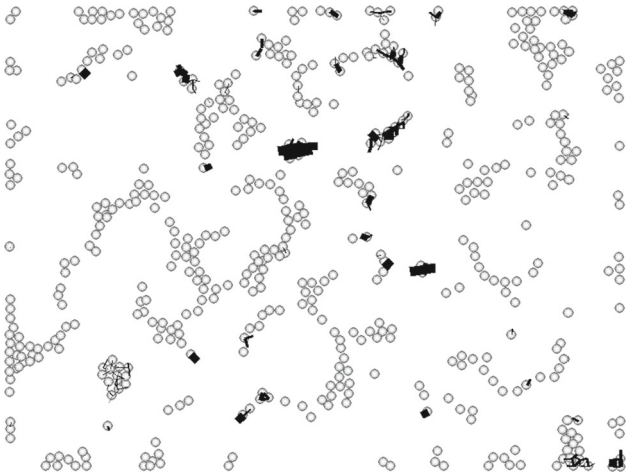

Fig. 5 Fines particles on the central plane of the dense sample of 10 % fines content at high stress level; *lines* indicate contact forces between fines particles where *line thickness* represent force magnitude

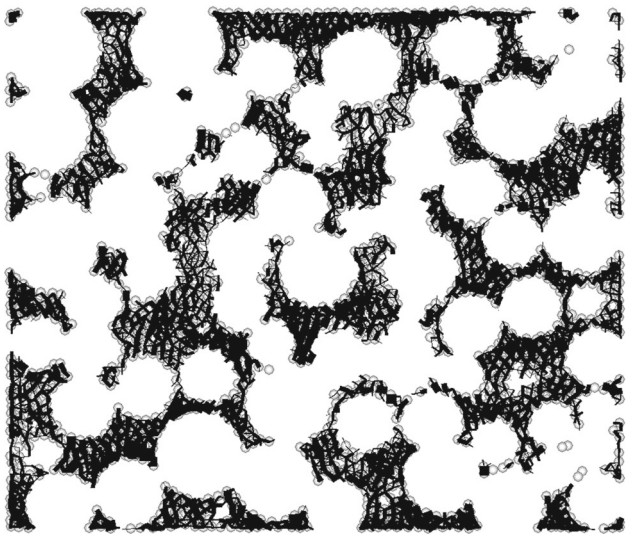

Fig. 6 Fines particles on the central plane of the dense sample of 30 % fines content at high stress level; *lines* indicate contact forces between fines particles where *line thickness* represent force magnitude

ticles force networks are not shown). The results in Figs. 4, 5 and 6 also agree with the results in [12] where we studied the contributions of each contact type categorised by different particle sizes in granular mixtures and how each contact network contributes to the overall deviator stress of the whole mixture sample. For samples of 10 % fines content, the overall deviator stress is almost entirely due to contacts between sand and sand particles. However, all contact network types have significant contributions to the deviator stress for 30 % fines. More details will be given in Sect. 4.2.

3.2 Microstructural properties of granular systems under 1D compression

The packing structure of a granular system can be investigated mathematically using the radial distribution function that gives the possibility of finding two particles at a distance r apart from each other. Figure 7 plots the radial distribution functions (*rdf*) of the fine particles subsystem of the samples of 100, 10 and 30 % fines contents at a "low stress level" of 5 MPa where $g(r)$ is a density value calculated as the number of the particles within a shell of a thickness Δr at a distance r away from a particle centre divided by the volume of the shell and normalized by the overall density of the whole system. A variation in the *rdf* reflects changes in the packing structure.

At the low stress level for the samples of 100 % fines, the *rdf* curves have a first peak at $r = d_0$ where d_0 is the diameter of the fine particles and the 2nd and the 3rd peaks at approximately $\sqrt{3}$ and 2 of d_0, which are the typical results for a monodisperse granular system that is close to jamming transition [15].

At the high stress level shown in the inset, the first peaks of all the samples are generally lower than those at the low stress level, and the curves are shifted to the left. These are due to a reduced relative distance between particles due to the densification effect of the compression. The *rdf* curves of the loose samples are not shown in Fig. 7 as they are similar to the dense samples although there are significant differences between these samples in terms of the solid fraction and of the percentage of the fine particles as rattlers.

The *rdf* of the fine particles of the 30 % fines sample is similar to that of the 100 % fines sample whereas the result of the 10 % fines sample is different, reflecting a significant change in the packing structure for the case with 10 % fines. Evidence of different packing structures has been shown in Figs. 5 and 6 in which the fine particles of the 10 % fines sample are mostly rattlers whereas the fine particles of the 30 % fines sample are non-rattlers and they participate in a percolating force network spanning across the sample.

Another microstructural signature of a granular packing going through the jamming transition can be reflected in the probability distribution function (*pdf*) of the contact forces between particles [3]. The *pdf* curves in this study were

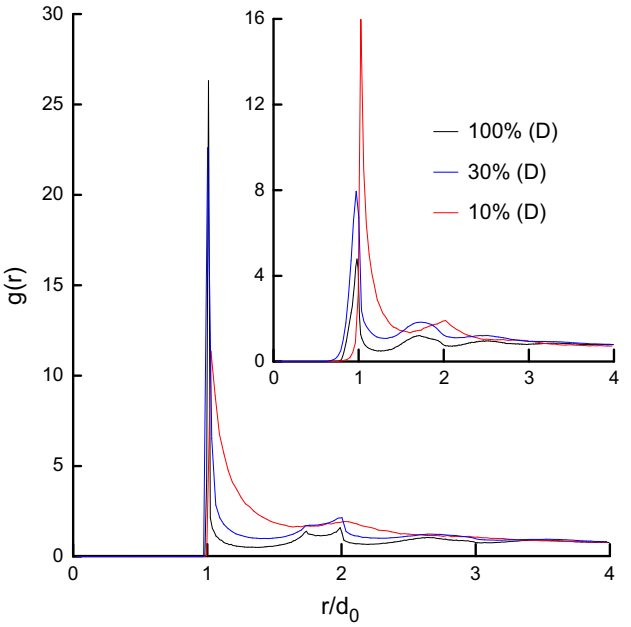

Fig. 7 Radial distribution functions of the fine particles subsystem *in* the 100, 30 and 10 % fines content of dense samples (D) at low stress levels; the inset shows the *rdf* (s) at high stress levels; results of loose samples are similar and not shown for clarity

obtained with the abscissa values calculated as the normal contact forces normalized by the mean normal contact force value in the system $\langle f_n \rangle$. The contact forces larger than $\langle f_n \rangle$ are strong forces that form the major force-bearing microstructures that tend to be oriented parallel to the loading direction whereas forces smaller than $\langle f_n \rangle$ are weak forces that tend to be approximately perpendicular to the loading direction and act as support for the strong force chains [5,6]. The shape of the *pdf* curves of the 0 % fines (shown in Figs. 16 and 18) resembled the typical *pdf* curve of a granular system in jammed state [3] with an exponential decay at large forces and the existence of a peak density value; this is different with the *pdf* curve of a granular system in an unjammed state that does not have a peak value and the probability densities decrease monotonically from the highest value that is located close to the vertical axis. The shape of the *pdf* curves of the 0 % fines samples obtained in this study does not change significantly at higher stress levels and this agrees with the results in [3] that the shape does not change as long as unjamming does not occur.

Particles can be separated into two groups of the particles that transmit at least one strong force (termed "involved particles"), and the other group of the "uninvolved particles" that only transmit weak forces [10]. Minh and Cheng [10] studied the evolution of the size distribution of the involved particles (referred to as sn_psd) and found that when the compression curves of samples with different initial densities converge, the sn_psd curves of the respective samples also follow a

convergence trend. The convergence of the *pdf* curves that occur simultaneously with the convergence of the sn_psd(s) could be a signature of an emerged common structure for the loose and dense samples at high stresses [19]. The contact force distributions of the 0 % fines samples in this study were similar at high stress levels regardless of the initial densities and the sn_psd of these samples showed that most of the particles were involved in the strong force transmission.

In our previous studies on granular mixtures, in which the fine particles added to the same host sand were varied in a systematic way [12,20], it was found that depending on the fines contents, the effects of polydispersity on the mixture behaviour can be categorized into three groups of the samples of the low fines contents (10–20 %), of the intermediate fines contents (30–50 %) and of the large fines contents (70–90 %). While the behaviour of the low and large fines content samples are dominated by the respective larger particle populations in each case, the behaviour of the intermediate fines content samples are influenced by both populations of the fine and the sand particles as no population is overly dominant in these systems.

For mixtures, contacts between the big and the small particles may contribute differently to the overall stress tensor depending on whether there are sufficient particles to form percolating force chains. The percolating force chains and the peak density in the *pdf* of contact forces are indications of a jammed system [1,3]. Figure 8 shows the abscissa positions of the peak densities in the *pdf(s)* of the mixtures as a function of the fines content. The results were obtained from the (overall) contact force distributions of all the interparticle contacts in the systems and from the individual force distributions of different contact types of b_b, b_s and s_s (see Eq. 1). At low stress levels, the overall *pdf(s)* of the low fines contents (10–20 %) reflect the results of unjammed systems with no peak density ($(f_n/\langle f_n\rangle)_{peak}$ is zero) and a monotonically decreasing *pdf*, which are due to the effects of the b_s and the s_s networks; the b_b network on the hand is jammed and the peak density is at the same position as with the 0 % fines. For the samples of intermediate and large fines contents, there are more small particles to form percolating strong force chains between them and the *pdf(s)* of the b_s and s_s networks now have the typical *pdf* shape of a jammed system with a peak density at the same position with the 0 % fines and 100 % fines; the b_b network however has different peak positions when the big particles lose the dominant role in transmitting contact forces in these samples.

The next section will discuss more in details the effect of the particle size polydispersity and of the vertical stress level on the contact force distribution and the packing structure of granular mixtures of the low and the intermediate fines content behaviour. Note that the behaviour of the large fines contents samples (e.g., 90 %) are similar to that of the low fines contents (e.g. 10 %) but with the fine particles dominant

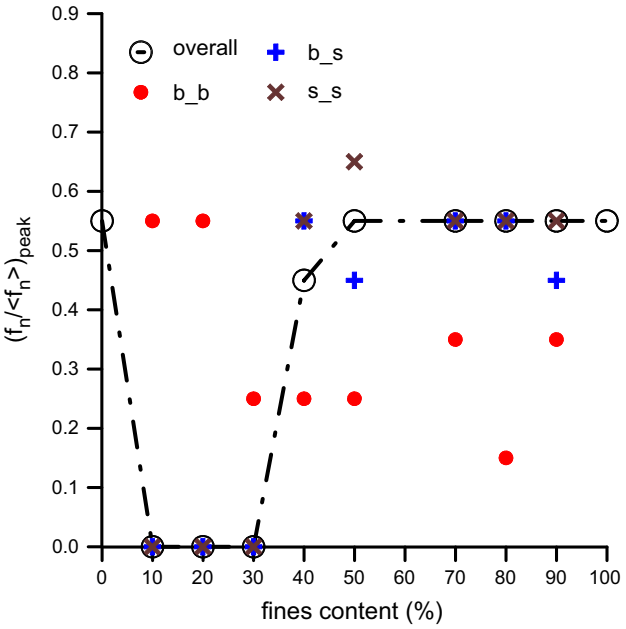

Fig. 8 Abscissa positions of the peak stresses of the contact force distribution of different contact types of dense mixtures at low stress levels

instead of the sand particles in terms of the major contribution of the contact forces induced by these particles to the deviator stress [12].

4 Contact force distributions of granular mixtures

While the *pdf* of contact forces is more sensitive to interparticle spatial correlation than the *rdf* as a small change in interparticle distance could lead to a big change in contact force [3], both curves are dependent on the polydispersity of a granular system. The macroscopic stress-strain behaviour of a sample depends on the strong forces as the deviator stress in a system is solely due to the contributions of these forces [5,6] and this is also a function of the polydispersity [12]. Bi et al. [1] studied the percolation of the clusters of the particles involved in the strong force transmission and associated it with the structural change at the jamming transition, here we studied the effect of polydispersity on the clusters of the involved particles and of the uninvolved particles as a function of the compression stress.

4.1 Structures of the best packing efficiency mixtures

Figure 9 shows the contact force distributions and the sn_psd curves of the 30 % fines samples at low stresses. For the dense sample there are approximately two thirds of the fine particles participating in the strong forces transmission as shown in the inset, whereas for the loose sample there is a negligible contribution from the fine particles. The *pdf* curves of the

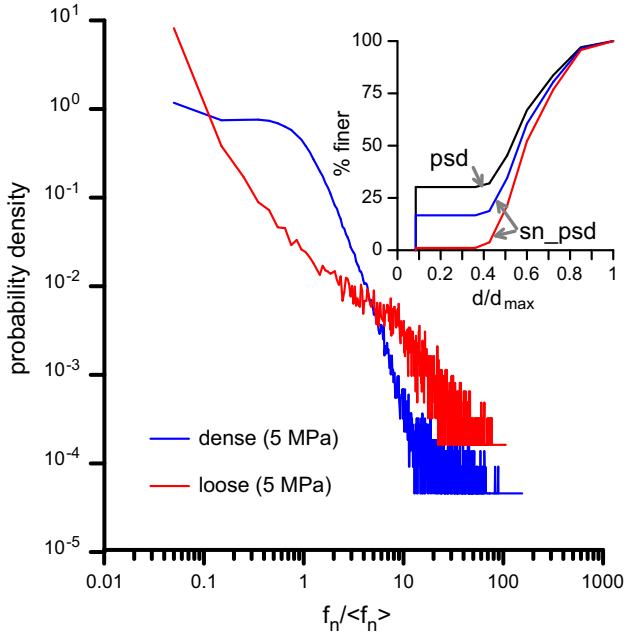

Fig. 9 Probability distributions of contact forces of 30 % fines content samples at low stress level; inset shows the overall particle size distribution *(psd)* and the *psd*(s) of the involved particles (sn_psd)

two samples are different, which reflects different packing structures as shown in Fig. 10 for the packing structures of the loose and dense samples of 30 % fines at low stresses. In Fig. 10b, as nearly all the fine particles are the uninvolved particles, they form the major part of the uninvolved clusters; among them about 70 % are rattlers as shown in Fig. 4, the remained 30 % mostly transmit weak forces. In Fig. 10a, the smaller clusters of the uninvolved particles are located within the central region of the sample while bigger clusters are located in the corners nearer to sample's boundaries; this could be due to the effect of the wall boundary condition that affects the force transmission through the granular sample.

At high stress levels in Fig. 11, the sn_psd and the pdf curves converge, which could be the signature for an emerged common structure as shown in Fig. 12 when the packing structures of the dense and loose samples are very similar. The uninvolved clusters are disconnected and distributed randomly for both samples, while the clusters of the involved particles that contain both big and small particles percolate in both directions representing a jammed system as was also observed in [1]. Note that not only the packing structures are similar in Fig. 12a, b but the proportions of the involved and the uninvolved particles are actually identical for the two samples as evidenced in the inset of Fig. 11. The similar packing structures in Fig. 12a, b are of two different random granular systems when they have the same solid fractions and boundary stresses.

A common packing structure emerges when the contact force distributions of different samples converge; the common packing structure can be described by two populations of the involved particles and of the uninvolved particles where the involved particles form percolating clusters across the sample and the uninvolved particles form isolated clusters within the dominant network of the other particles population.

4.2 Micro-characteristics of individual contact networks

Figure 13 shows the contributions of different contact types depending on the sizes of two contacting entities to the macroscopic deviator stress $\sigma_d (= \sigma_1 - \sigma_3)$ at high stresses (further information on the method of calculation is given in

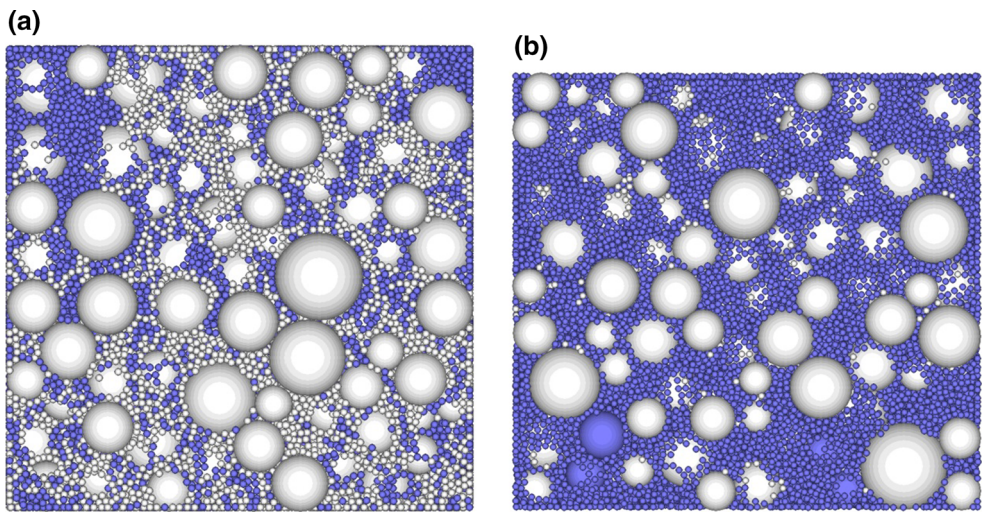

Fig. 10 Particles involved (*white*) and not involved (*blue*) in the transmission of strong contact forces within a thin 1 mm central vertical slice at low stress level for samples of 30 % fines content. **a** Dense, $\sigma_v = 5$ MPa, width = 6.073 mm, **b** Loose, $\sigma_v = 5$ MPa, width = 6.296 mm (colour figure online)

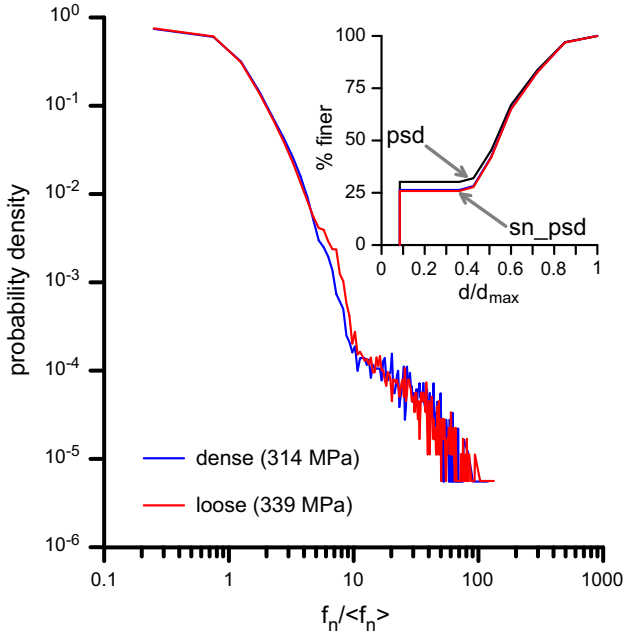

Fig. 11 Probability distributions of contact forces of 30 % fines content samples at high stress level; inset shows the overall particle size distribution *(psd)* and the *psd*(s) of the involved particles (sn_psd)

[12]). Although all three contact types have significant contributions, the b_s contacts between the big (b) sand particles and the smaller (s) fine particles have the largest contribution to the deviator stress, which is followed by the b_b contacts and finally the s_s contacts that have the smallest contribution. The dense and loose samples have identical overall deviator stress values as well as identical individual contributions for different contact types. When we normalized the curves in Fig. 13 by dividing the ordinate values by the maximum value of σ_d of each curve and dividing the abscissa values by the average normal contact force of each contact type, the curves in Fig. 13 collapse into a very narrow band as shown in Fig. 14. The results of the 0 % fines samples, which are of b_b contacts, are also included for comparison with the results of mixture samples. The curves cross the horizontal axis similarly at approximately unity abscissa value; this means that each contact network (b_b, b_s and s_s) is comprised of its own strong contacts and weak contacts that is similar to the force transmission behaviour of the 0 % fines samples (the results of 0 and 100 % are similar to each other [12]).

Figure 15 shows the percentage values of the cumulative number of contacts of different contact types with increasing magnitudes, the ordinate value at unity abscissa is approximately 61 %. The percentage of the strong contacts is hence 39 % whereas the percentage of the weak contacts is 61 % for different contact networks of the 30 % fines samples and of the 0 % fines samples. These values result in a ratio of 1.56 between the number of weak contacts over the number of strong contacts and a ratio of 1.64 between the total number of contacts over the number of weak contacts for different contact networks, which are close to "the golden ratio" of 1.62 [21].

The particle stiffness was set proportional to particle radius [10,12,14]; the *pdf* of all contact forces in Fig. 11 could be in general comprised of three parts where the smallest forces are the s_s forces, followed by the bigger b_s forces and the biggest b_b forces with possible overlaps between them. Figure 16 shows the pdf of different contact types for 30 % fines and 0 % fines. When normalized by its own average normal force value, each contact network has a pdf curve that is similar to the pdf of the 0 % fines samples, which has been described as a typical pdf curve for a jammed granular system. Note that the results in Figs. 13, 14, 15 and 16 are independent of the initial density for both sand samples and mixture samples which proves that a common packing structure was attained in each case.

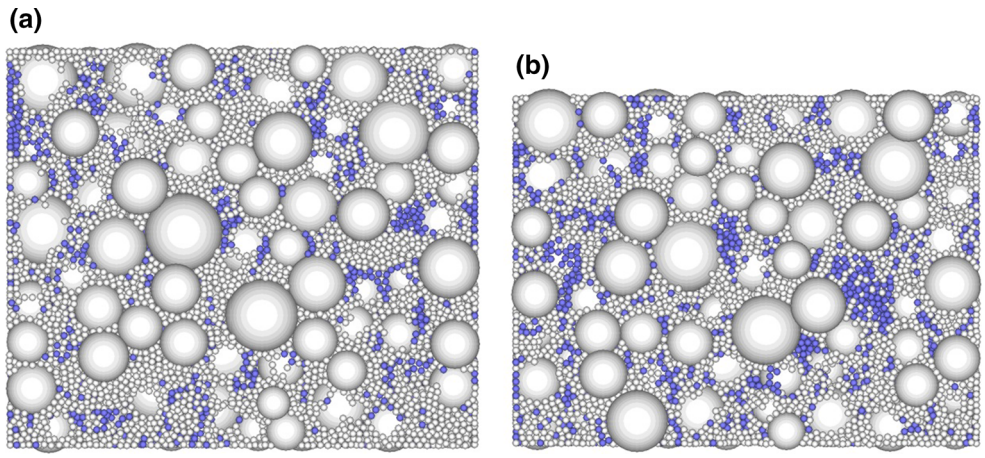

Fig. 12 Particles involved (*white*) and not involved (*blue*) in the transmission of strong contact forces within a thin 1 mm central vertical slice at high stress level for samples of 30 % fines content. **a** Dense, $\sigma_v = 314$ MPa, width = 6.073 mm, **b** Loose, $\sigma_v = 339$ MPa, width = 6.926 mm (colour figure online)

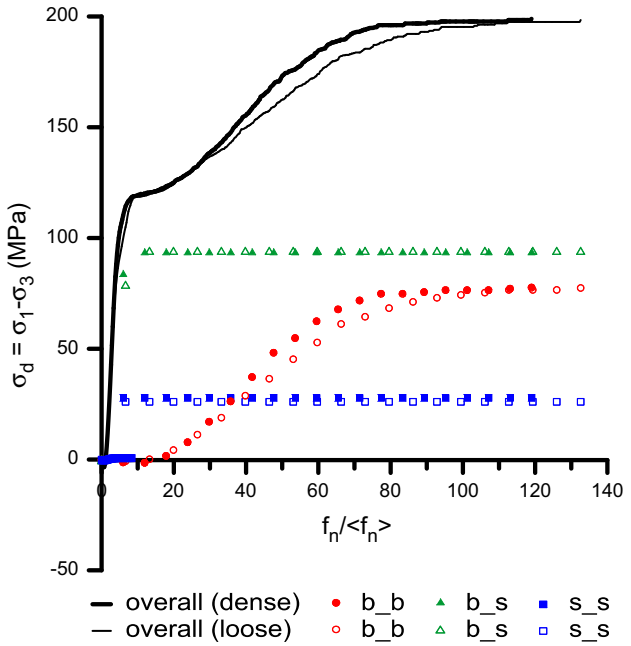

Fig. 13 Cumulative contribution of the contact network to the overall deviator stress for dense and loose samples of 30 % fines contents at high stress levels

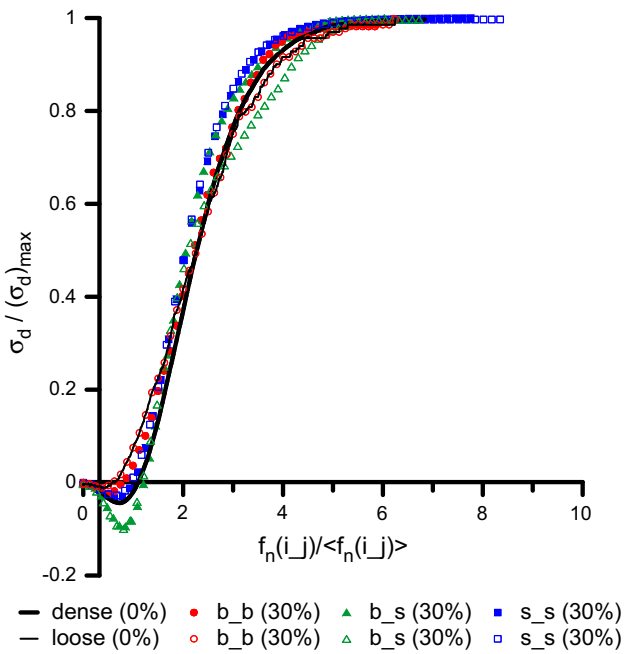

Fig. 14 Normalized cumulative contribution of the contact network to the deviator stress for dense and loose samples of 0 % (*line*) and 30 % (*symbol*) fines contents at high stress levels; f_n(i_j) indicates the contact forces of different types where i_j can be b_b, b_s or s_s

A common packing structure was attained at high stresses for 0 % fines and for 30 % fines in each case but they are very different from each other due to different particle size distributions. Nevertheless, the results in Figs. 14, 15 and 16 also show that there is similarity between the 0 % fines and the 30 % fines samples. When the particle population of a component material in a granular mixture significantly participates in the transmission of forces, which can be described in terms of the non-rattler fraction as in Fig. 4, they form part of a percolating cluster comprised of the involved particles in the system and these particles are jammed. The probability distributions of the contact forces of the jammed particles follow a typical curve as shown in Fig. 16 with a narrow particle size distribution. The contact force distribution is not only the structural signature of jamming in a granular system [3] but it is also a signature for the jamming of a subsystem of certain particle sizes in a granular mixture.

4.3 Force distributions in the low-fines-content-mixtures

Figure 17 shows the pdf and the sn_psd of the 10 % fines samples at high stresses; the curves of the dense and the loose samples converge, similar to the results in Fig. 11, which reflects a common packing structure that is independent of the initial densities. The sn_psd(s) show that nearly all the fine particles are not involved in the percolation of the strong force chains and according to the discussion above the subsystem of fine particles in these samples are not in a jammed state.

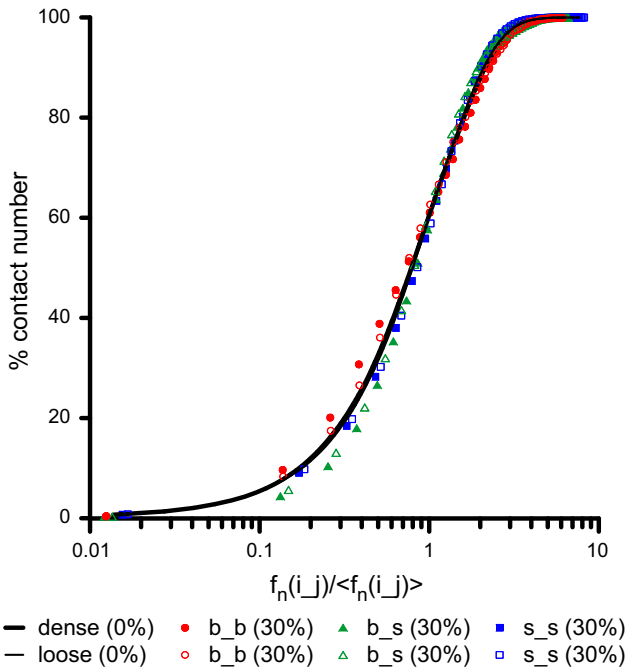

Fig. 15 Cumulative percentage of contact numbers of different types for dense and loose samples of 0 % (*line*) and 30 % (*symbol*) fines contents at high stress levels; f_n(i_j) indicates the contact forces of different types where i_j can be b_b, b_s or s_s

Figure 18 shows the pdf curves of the b_s and the s_s contact forces and of the b_b contact forces in the inset in comparison with the pdf of the 0 % fines samples. There are

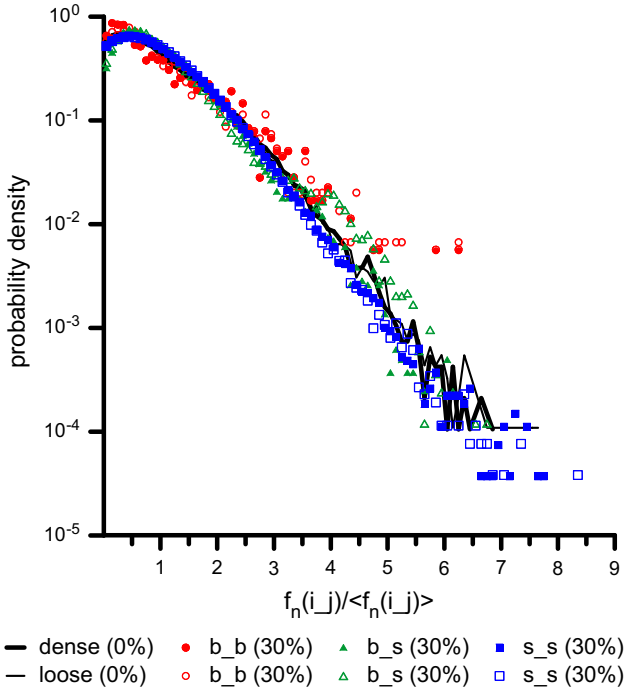

Fig. 16 Probability force distributions of different contact types for dense and loose samples of 0 % (*line*) and 30 % (*symbol*) fines contents at high stress levels; f_n(i_j) indicates the contact forces of different types where i_j can be b_b, b_s or s_s

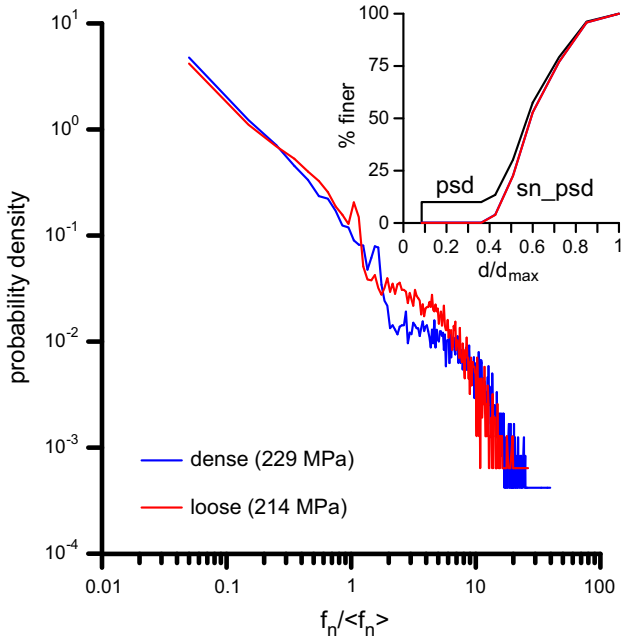

Fig. 17 Probability distributions of contact forces and particle size distributions of 10 % fines content samples at high stress levels

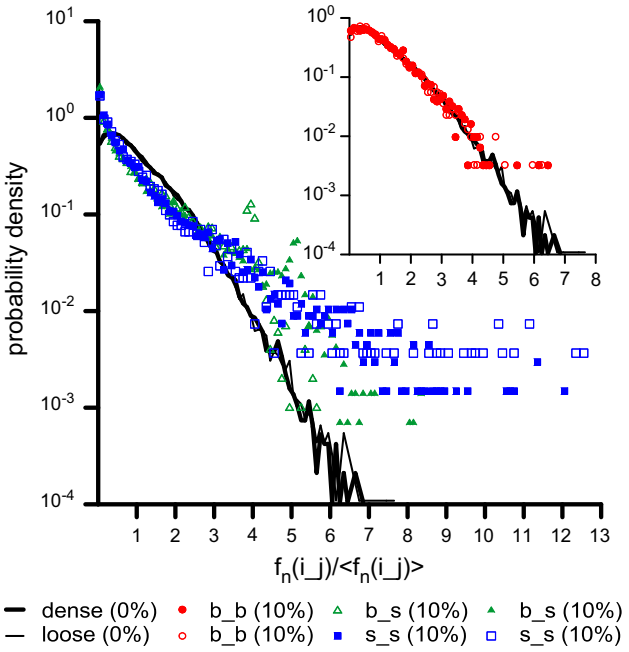

Fig. 18 Probability force distributions of different contact types for dense and loose samples of 0 % (*line*) and 10 % (*symbol*) fines contents at high stress levels; fn(i_j) indicates the contact forces of different types where i_j can be b_b, b_s or s_s

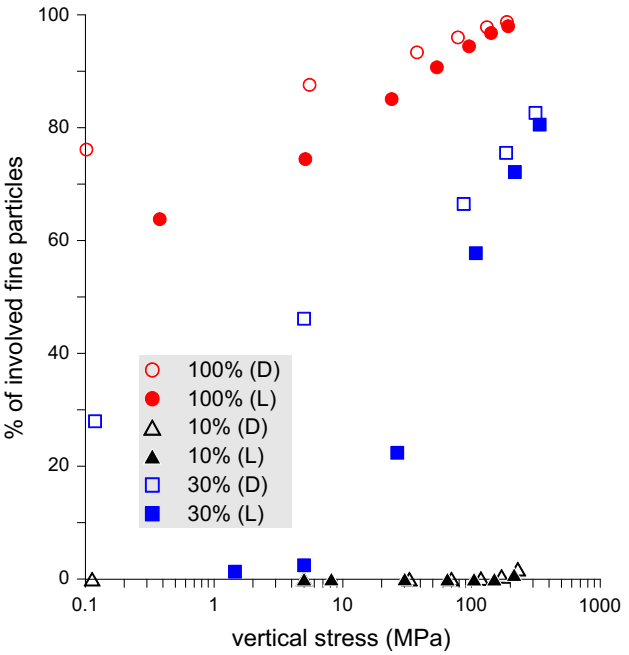

Fig. 19 Percentage of the fine particles that are involved in the transmission of strong forces

striking differences between the curves in the main plot and in the inset. As the big sand particles are the involved particles, their contact force distribution is of a jammed system that agrees very well with the curves of the 0 % fines. The pdf(s) of the b_s and the s_s contacts on the other hand are similar to the results of an unjammed system with no peak density value and the probability density values decreases monotonically with increasing force values; this confirms the results in Fig. 17.

The percentage of the fine particles that transmit strong forces are plotted against the vertical stress values in Fig. 19 for samples of uniform particle sizes, of low fines content and of intermediate fines content. Dense and loose samples achieve the same percentage values at high stresses. The convergence is slower but with better final convergence (same percentage value at the final stresses) compared to the results in Fig. 4 where there is about 10 % difference in the non-rattler percentages between the loose and dense samples of 10 % fines content at the final stress. The percentage of the involved fine particle can be used as an indicator for the jamming of the fine particle population in granular mixtures. The fraction of the uninvolved fine particles can be considered as void in the calculation of the equivalent granular void ratio (e^*) for the systems of low fines contents (10–20 % fines) [20]. The compression curves in terms of e^* and the vertical stress of these samples coincide showing similar behaviour that mixtures of low fines contents are dominated by the sand particles subsystem.

5 Conclusions

We have studied one dimensional compression behaviour of granular mixtures using the Discrete Element Method to investigate the distributions of contact forces between particles of different sizes and found that a common packing emerged at high stresses that is independent of the initial density of the sample. The common packing structure can be detected when a common probability distribution of contact forces is obtained for samples of different initial densities. The effect of polydispersity on the common packing structure can be described in terms of the particle size distribution of the particles involved in the strong force transmission in the system. For granular mixtures of a wide particle size distribution, when the particle population of a component material significantly participates in the transmission of forces, they form parts of a percolating cluster comprised of all the involved particles in the system and these particles are jammed and their contact force distributions are of a jammed system that has a peak probability density near to the average force value and an exponential tail at higher force values. For systems of a small percentage of the fine particles, the fine particles do not actively participate in the strong force transmission and the shape of the pdf curves related to the fine particles population reflects the characteristic of an unjammed state for the subsystem consisted of these particles. The contact force distribution is hence not only the structural signature of jamming in a granular system [3] but it is also a signature for the jamming of a subsystem of certain particle sizes in a granular mixture.

Acknowledgments The first author gratefully acknowledges the financial support of Nazarbayev University, Kazakhstan for the collaboration in this work and we would like to thank Dr. Colin Thornton and the anonymous reviewers for their valuable suggestions.

References

1. Bi, D., Zhang, J., Chakraborty, B., Behringer, R.P.: Jamming by shear. Nature **480**(7377), 355–8 (2011). doi:10.1038/nature10667
2. Liu, A.J., Nagel, S.R.: Jamming is not just cool any more. Nature **396**, 21–22 (1998)
3. Corwin, E.I., Jaeger, H.M., Nagel, S.R.: Structural signature of jamming in granular media. Nature **435**(June), 1075–1078 (2005). doi:10.1038/nature03698
4. Kumar, N., Luding, S.: Memory of jamming–multiscale flow in soft and granular matter. arXiv:1407.6167v2 [rcond-mat.soft] (2015)
5. Radjai, F., Wolf, D., Jean, M., Moreau, J.J.: Bimodal character of stress transmission in granular packings. Phys. Rev. Lett. **80**, 61–64 (1998)
6. Thornton, C., Antony, S.J.: Quasi-static deformation of particulate media. Philos. Trans. R. Soc. A **356**, 2763–2782 (1998)
7. Lade, P.V., Yamamuro, J.A.: Effects of nonplastic fines on static liquefaction of sands. Can. Geotech. J. **34**(6), 918–928 (1997)
8. Carrera, A., Coop, M., Lancellotta, R.: Influence of grading on the mechanical behaviour of Stava tailings. Géotechnique **61**(11), 935–946 (2011)
9. Minh, N.H., Cheng, Y.P. One dimensional compression of gap-graded mixtures in DEM. In: Proceedings of the International Symposium on Geomechanics and Geotechnics: From Micro to Macro, pp. 727–731. Shanghai (2010)
10. Minh, N.H., Cheng, Y.P.: A DEM investigation of the effect of particle-size distribution on one-dimensional compression. Géotechnique **63**, 44–53 (2013)
11. Altuhafi, F.N., Coop, M.R.: Changes to particle characteristics associated with the compression of sands. Géotechnique **61**(6), 459–471 (2011)
12. Minh, N.H., Cheng, Y.P., Thornton, C.: Strong force networks in granular mixtures. Granul. Matt. **16**, 69–78 (2014). doi:10.1007/s10035-013-0455-3
13. Shire, T., O'Sullivan, C., Hanley, K.J., Fannin, R.J.: Fabric and effective stress distribution in internally unstable soils. J. Geotech. Geoenviron. Eng. **140**(12), 04014072 (2014)
14. Itasca Inc.: Particle Flow Code in 3 Dimensions (PFC3D) Version 4. Minnesota, USA (2008)
15. Zhang, H., Makse, H.: Jamming transition in emulsions and granular materials. Phys. Rev. E **72**(1), 011301 (2005). doi:10.1103/PhysRevE.72.011301
16. Baranau, V., Tallarek, U.: Random-close packing limits for monodisperse and polydisperse hard spheres. Soft Matt. **10**(21), 3826–3841 (2014). doi:10.1039/c3sm52959b
17. Chan, S.H., Ngan, A.H.W.: Statistical distribution of contact forces in packings of deformable spheres. Mech. Mater. **37**(4), 493–506 (2005)
18. Thornton, C.: Numerical simulations of deviatoric shear deformation of granular media. Géotechnique **50**(1), 43–53 (2000)
19. Minh, N.H., Cheng, Y.P.: Micro-characteristics of monodisperse and best-packing mixture samples under one dimensional compression. AIP Conf. Proc. **1542**, 265 (2013)
20. Minh, N.H., Cheng, Y.P. A micromechanical study of the equivalent granular void ratio of soil mixtures using DEM. In: Proceedings of the International Symposium on Geomechanics and Geotechnics: From Micro to Macro, pp. 219–224. Cambridge (2014)
21. Olsen, S.: The Golden Section: Nature's Greatest Secret. Walker Publishing Company, New York (2006)